Construction and Building Materials 113 (2016) 864–869

Contents lists available at ScienceDirect

Construction and Building Materials

journal homepage: www.elsevier.com/locate/conbuildmat

Evaluate orthotropic properties of wood using digital image correlation

Gi Young Jeong [a,*], Moon Jae Park [b]

[a] Chonnam National Univ. Dept. of Wood Science and Engineering, Gwangju, Republic of Korea
[b] Korea Forest Research Institute, Seoul, Republic of Korea

HIGHLIGHTS

- Elastic properties and ratios from four different wood materials were determined.
- Poisson's ratio from four different wood materials was determined.
- Strength and failure behavior from four different wood materials were determined.
- Off-axis tension test with DIC was used to evaluate the orthotropic properties.

ARTICLE INFO

Article history:
Received 18 November 2015
Received in revised form 8 March 2016
Accepted 23 March 2016
Available online 28 March 2016

Keywords:
Orthotropic property
Wood
Digital image correlation
Shear strength
Elastic modulus

ABSTRACT

The goal of this study is to evaluate the orthotropic properties of four different wood species. Off-axis tension tests with digital image correlation were used to evaluate the orthotropic properties of *Larix kaempferi*, *Pinus densiflora*, *Pinus koraiensis*, and *Cryptomeria japonica*. The highest elastic modulus E_L of 11.70 GPa was found from *Larix kaempferi*, whereas the lowest elastic modulus E_R of 0.12 GPa was observed from *Cryptomeria japonica*. The highest shear modulus G_{LT} of 2.68 GPa was found from *Larix kaempferi* and the lowest shear modulus G_{LR} of 0.32 GPa was observed from *Cryptomeria japonica*. While the shear modulus values in the LT plane from the four species were higher, the shear strength values in the LR plane were higher than those in the LR plane. Poisson's ratios from the four species were found that ν_{RT} and ν_{TR} were higher than ν_{LR} and ν_{LT}. Although mixed failure behaviors were found from the four species, the failure behaviors were dominantly influenced by the orientation of the specimens.

1. Introduction

Wood is normally defined as an orthotropic material at the macro scale. Previous studies have demonstrated the orthotropic properties of many different wood species (Hearmon [1], Goodman and Bodig [2], Bodig and Goodman [3], Gunnerson et al. [4], Sliker [5], and Jeong et al. [6]). The orthotropic properties of different orientation boards from different species were evaluated using plate theory by Hearmon [1]. Gunnerson et al. [4] proposed an alternative beam theory in the measurement of the elastic modulus of wood materials instead of the plate theory proposed by Hearmon [1]. The alternative beam theory associated with a correction factor was used to rotate the beam axis to adjust deflection, which was overestimated by the two-way bending effect (Goodman and Bodig [2], Bodig and Goodman [3], and Gunnerson et al. [4]). However, it is unclear how the corrected elastic modulus can be applied to evaluate Poisson's ratio of different wood species. Most of the orthotropic properties of wood materials were available today evaluated from the methods (Bodig and Goodman [3]).

Digital image correlation (DIC) has been used to measure the mechanical properties of wood materials (Serrano and Enquist [7], Ljungdahl et al. [8], Konnerth et al. [9], Jeong et al. [10], and Jeong et al. [6]). To obtain reliable elastic modulus and Poisson's ratio of wood materials using DIC, the effects of the loading rate and thickness on the elastic properties of wood were evaluated (Jeong et al. [11]). The effects of different window sizes, speckle patterns, and light on elastic modulus of wood were analyzed (Jeong et al. [10]). DIC was found to be one of the reliable methodologies for the measurement of the orthotropic properties of wood materials. DIC could characterize the full field strain distribution and quantify the two-dimensional strain behavior. The elastic properties, including elastic modulus, shear modulus, and Poisson's ratio can be quantified from the two dimensional strain behavior using DIC.

Therefore, in this study, the direct determination of the orthotropic properties of larch, red pine, nut pine, and Japanese cedar was conducted using off-axis tension tests with DIC. A series

* Corresponding author.
E-mail address: gjeong1@jnu.ac.kr (G.Y. Jeong).

http://dx.doi.org/10.1016/j.conbuildmat.2016.03.129
0950-0618/

of images was captured for the strain measurement and was synchronized with loading data for the calculation of the elastic modulus and Poisson's ratio. The ultimate tensile strength (UTS) and shear strength were also measured.

2. Materials and Methods

Three logs each from *Larix kaempferi*, *Pinus densiflora*, and *Pinus koraiensis* from the Kwangwon province and three logs from *Cryptomeria japonica* from the Jeju island in South Korea were used in this study. A minimum of three trees from each species were cut for the preparation of the differently oriented specimens (Fig. 1). Stems were cut in half through the pith area to generate different planes of wood blocks. A minimum of thirty dog-bone shape specimens were prepared for the mechanical properties.

Fig. 1 shows the three axes of the longitudinal (L), the radial (R), and the tangential (T) directions and earlywood layers in white and latewood layers in grey. The longitudinal direction is parallel to the fiber direction. The radial and tangential directions are transverse to the fiber direction. The radial direction is perpendicular to the growth ring and parallel to the ray cells. The tangential direction is tangent to the growth ring but normally the longitudinal and radial directions are defined first and the tangential direction is determined. Six differently oriented specimens were cut from each plane. From the longitudinal-radial plane, (a) longitudinal-radial (LR), (b) LR angled specimens were prepared. From the longitudinal-tangential plane, (c) longitudinal-tangential (LT), (d) LT angled specimens were prepared. From the radial-tangential plane, (e) radial-tangential (RT), and (f) tangential-radial (TR) specimens were prepared. For the evaluation of the shear modulus and shear strength, longitudinal-radial angled and longitudinal-tangential angled plane specimens were cut to 30° from the longitudinal direction. All specimens were conditioned to stabilize at 6% equilibrium moisture content in the environment chamber for 1 month before testing.

Tension tests used a universal testing machine equipped with a 150 kN load cell. The loading rate of 0.5 mm/min and a gage length of 10 cm were used to measure the material properties of the differently oriented specimens.

Fig. 2 shows the two cameras used for the DIC. The strain measurement was obtained from DIC. The camera set up for DIC and synchronization for loading and strain used the same arrangement reported in a previous study (Jeong et al. [6] and Jeong et al. [11]). A sequence of images was captured during the test using the two CCD cameras. The CCD camera was mounted on a stand with a macro adjustable holder. When tension load was applied, the specimen was photographed at 20 frame rates. The distance between the lens and the object was adjusted to produce a clear image. A facet size of 15 and a facet step of 8 were used to analyze the displacement of specimen. The facet was generated on the digital image of the surface of the wood specimens (Fig. 3). The position of the facet was recorded as the x, y coordinate of the pixel position on the image.

The different elastic moduli from the differently oriented specimens were obtained using Eq. (1). Poisson's ratios were obtained from Eq. (2). Different ultimate tensile strengths (UTS) were obtained from Eq. (3). Shear moduli and shear strengths were obtained using Eqs. (4) and (5), respectively.

E_L, ν_{LR}, and σ_L were measured from the LR plane specimen. E_L, ν_{LT}, and σ_L were measured from the LT plane specimen. E_R, ν_{RT}, and σ_R were measured from the RT plane specimen. E_T, ν_{TR}, and σ_T were measured from the TR plane specimen.

$$E = \frac{\Delta P}{\Delta \varepsilon}\left(\frac{1}{A}\right) \tag{1}$$

$$\nu_{12} = \frac{\varepsilon_2}{\varepsilon_1} \tag{2}$$

Fig. 2. Digital image correlation testing set up showing two cameras, stereo plate, and tension specimens.

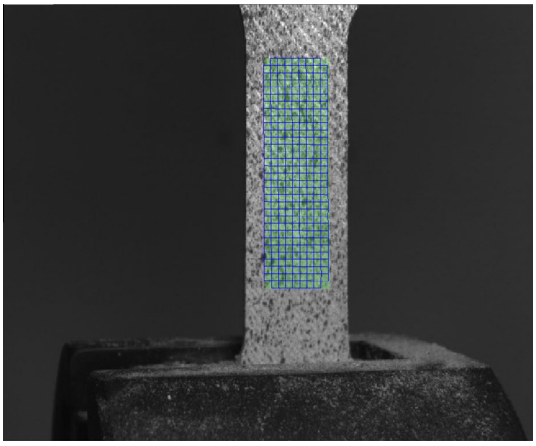

Fig. 3. Virtual grids generated on the surface of the specimens.

$$\mathrm{UTS} = \frac{P_{max}}{A} \tag{3}$$

$$G_{12} = \frac{1}{\left(-\frac{1}{E_1}cos^4\theta - \frac{1}{E_2}sin^4\theta + \frac{1}{E_\theta}\right)\frac{1}{sin^2\theta cos^2\theta} + \frac{2\nu_{12}}{E_1}} \tag{4}$$

$$\tau_{12} = \sigma_{max} sin\theta cos\theta \tag{5}$$

Where,

ΔP: Change of load
$\Delta \varepsilon$: Change of strain
A: Cross sectional area
P_{max}: Peak load

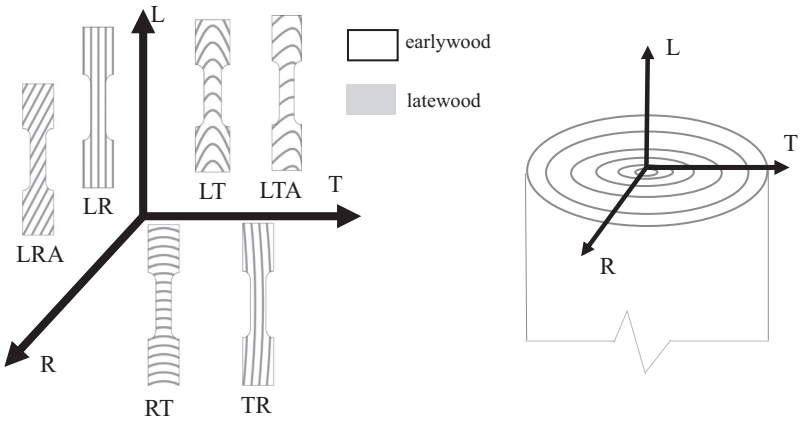

Fig. 1. Six differently oriented specimens along the three planes LR, LT, and RT.